Poisson effect driven anomalous lattice expansion in metal nanoshells

Ganesh Iyer, Suboohi Shervani, Gargi Mishra, Deb De, Arun Kumar, Sri Sivakumar, Kantesh Balani, Raj Pala, and Anandh Subramaniam

Citation: Appl. Phys. Lett. **110**, 131603 (2017); doi: 10.1063/1.4979460
View online: http://dx.doi.org/10.1063/1.4979460
View Table of Contents: http://aip.scitation.org/toc/apl/110/13
Published by the American Institute of Physics

Poisson effect driven anomalous lattice expansion in metal nanoshells

Ganesh Iyer,[1] Suboohi Shervani,[1] Gargi Mishra,[2] Deb De,[2] Arun Kumar,[1] Sri Sivakumar,[2] Kantesh Balani,[1] Raj Pala,[2] and Anandh Subramaniam[1,a)]
[1]*Department of Materials Science and Engineering, Indian Institute of Technology, Kanpur 208016, India*
[2]*Department of Chemical Engineering, Indian Institute of Technology, Kanpur 208016, India*

(Received 28 November 2016; accepted 11 March 2017; published online 30 March 2017)

Surface stress can have profound effects on nanoscale materials and can lead to a contraction of the lattice in nanoparticles to compensate for the under-coordination of the surface atoms. The effect of elastic properties like Poisson's ratio can be accentuated in lower dimensional systems. The current study focuses on hollow metal nanoshells (MNSs), wherein there is interplay between the surface stresses existing in the inner and outer surfaces. Using a two scale computational method and transmission electron microscopy, we not only show a lattice expansion (in the radial direction) due to purely surface stress effects in a metallic system but also discover anomalous lattice expansion in the case of very thin walled MNSs. We argue that this effect, wherein the stress in the outer surface causes expansion in the radial lattice parameter (instead of compression), is a Poisson effect driven phenomenon. Although Ni nanoshells are used as an illustrative system for the studies, we generalize this effect for all metal nanoshells. *Published by AIP Publishing.*
[http://dx.doi.org/10.1063/1.4979460]

Surface stress can have profound effects in regions close to the surface on bulk materials and on nanoscale materials. Experimental and theoretical methods have been used to study the reduction of the lattice parameter with the size of the freestanding (unconstrained) metallic nanocrystal.[1–3] While this contraction in the lattice parameter may depend on the crystal morphology (e.g., spherical, octahedral, and cubic shapes) and position within the nanocrystal,[4,5] the crystal contracts seem to be an unchallenged observation.[6]

The elastic behaviour of isotropic materials is dictated by two moduli: Poisson's ratio (ν) and the Young's Modulus (E or Y). Amorphous phases are truly isotropic, while polycrystalline materials with randomly oriented grains can be approximated to an isotropic material. For most elemental metals, Poisson's ratio varies in the range of 0.25–0.4; however, extreme values exist like that for Beryllium ($\nu = 0.02$) and Thallium ($\nu = 0.45$).[7] It is interesting to note that Poisson's ratio for materials can be positive, zero,[8] or even negative.[9,10] As expected, the value of Poisson's ratio plays an important role in the elastic behaviour of materials.[11] The effect of Poisson's ratio on a variety of phenomena has been investigated.[12–15]

In addition to fully dense nanoparticles, hollow nanostructures have been investigated in a variety of contexts. Carbon nanotubes, carbon onions, and clathrates are well studied among these.[16] Nanoshells are an important class of hollow nanostructures, which have been investigated in diverse contexts.[17–19]

The present investigation focuses on single phase hollow metal nanoshells (abbreviated as MNSs), wherein the interplay between the stress existing in the inner and outer surfaces determines the altered lattice parameter. In the current work using a two-scale computation and transmission electron microscopy (TEM) we (i) demonstrate the lattice expansion (in the radial direction) due to purely surface stress effects in a metallic system (thin walled MNSs), (ii) discover Poisson effect driven anomalous lattice expansion in very thin walled MNSs, and (iii) show that this phenomenon is expected to be universal for all MNSs. Ni is used as an illustrative system for the abovementioned points (i) and (ii) in the study. It is to be noted that spherical hollow nanoparticles have been used in the current work (as a "model system"), while in general, nanocrystals have "rounded" edges and vertices only above the roughening transition temperature (i.e., have a tendency to become spherical) and are polyhedral below this temperature.[20–22]

The computational method is based on the recently developed technique, which is briefly outlined here and the details (including validation) can be found elsewhere.[23] The surface stress is computed based on an idea originally proposed by Shuttleworth,[24] wherein a surface of atoms is brought into registry with the bulk via the imposition of biaxial eigenstrains. The idea is implemented using a two-scale simulation, wherein (i) the lattice parameter of a layer of atoms is determined using the density functional theory (DFT) and (ii) this value is used in a finite element model to compute the surface stress. The advantage of the methodology is that the inner and outer surface stresses can be simulated independently (or in combination), and correspondingly, their effects on the lattice parameter can be understood separately. The details of the computation can be found elsewhere (see supplementary material, Section 1.1). In case large deformations of the body are involved, the method of computation of surface stress as prescribed by Gurtin and Murdoch can be used.[25]

To compare the results of the computations with experiments, (i) Ni MNSs are synthesized by the hydrothermal method and (ii) lattice parameter is determined by high resolution lattice fringe imaging (HRLFI) in a transmission electron microscope (TEM). To compute the lattice parameter in

a)Author to whom correspondence should be addressed. Electronic mail: anandh@iitk.ac.in.

the radial direction (a_{radial}), fringes "running" normal to the radial direction are used to obtain the interplanar spacing (d_{hkl}), which is further used for the computation of the local value of a_{radial}.

The value of the interatomic spacing for a (111) monolayer of atoms of Ni as determined from the DFT is 2.484 Å, which serves as the input to the finite element model. Fig. 1 shows the variation of a_{radial} (measured at the middle of the shell) with a shell thickness (t) for a MNS (OD = 80 nm), as computed using the two-scale simulations. The horizontal dashed line corresponds to the lattice parameter of the bulk material ($a_{bulk}^{Ni} = 3.513$ Å). The effect of outer and inner surface stresses, separately and in combination on a_{radial}, is illustrated in the figure. These have been labelled a_{outer}, a_{inner}, and a_{net} in the figure. According to the classical viewpoint, the outer surface stress tends to compress the particle, which can lead to a decrease in a_{radial}. On the contrary, the inner surface stress has a tendency to expand a_{radial}. The horizontal dotted line corresponds to the lattice parameter of a 80 nm diameter nanoparticle ($a_{NP} = 3.511$ Å).

Three regimes can be identified in the plot (Fig. 1): (i) thick shell (R1), (ii) thin shell (intermediate shell thickness, R2), and (iii) very thin shell (R3). The thick shell regime is similar to that of a nanoparticle, wherein the effect of the outer surface stress dominates (over the inner surface stress), and there is a reduction in the a_{radial}. The thin shell case is converse of the thick shell case, wherein the inner surface stress dominates over the outer one, and this leads to an expansion in the lattice parameter (the transition from R1 to R2 occurs at a critical shell thickness of $t_n^* \approx 26$ nm). It is to be noted that in this regime, the outer surface stress leads to a compression, which is as expected. The interesting and unexpected features of the figure are the crossover of a_{bulk}^{Ni} with a_{outer} (at a critical shell thickness of $t_o^* \approx 20$ nm). At a shell thickness below this value, the outer surface stress anomalously leads to an expansion of the lattice parameter (a_{radial}). Needless to say, this will lead to an enhanced

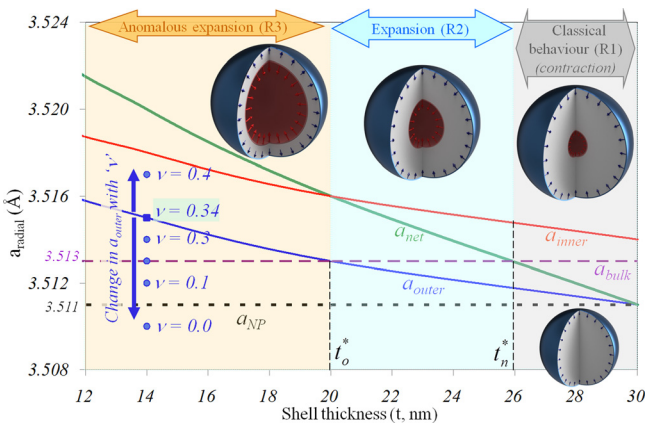

FIG. 1. Variation in the radial lattice parameter (a_{radial}) with the shell thickness for a nanosphere of Ni with OD = 80 nm computed using a two-scale method. The influence of outer, inner, and combined surface stresses on the lattice parameter is shown separately (a_{outer}, a_{inner}, and a_{net}). The lattice parameter for a shell thickness of 14 nm for varying values of ν (0–0.5) is also overlaid. The dashed line corresponds to the bulk lattice parameter (a_{bulk}^{Ni}) and the dotted line to the lattice parameter of a nanoparticle (a_{NP}). The inset shows the schematic of shells and nanoparticle and the effect of surface stress on the lattice parameter (as arrow marks).

increase in a_{radial}, as now both a_{inner} and a_{outer} leads to a lattice parameter expansion. To understand the reason for this effect and to demonstrate that it is driven by the Poisson effect, we artificially vary Poisson's ratio (ν) in the simulations. For a value of the shell in the range R3 (OD = 80 nm; t = 14 nm), a_{outer} is computed for a few values of "ν" ($\nu = 0.0$, 0.1, 0.2, 0.3 and 0.4) and overlaid on Fig. 1. The values of Poisson's ratio spans a range around the natural value for Ni ($\nu_{Ni} = 0.34$). It is observed that when the Poisson's ratio is set to a value below 0.2, the expected behaviour for the outer surface stress (i.e., leading to a compression of a_{radial}) is retrieved. On the other hand, if Poisson's ratio is increased above ν_{Ni} (= 0.34), the anomalous effect (i.e., expansion of the lattice parameter due to the outer surface stress) is even more accentuated. This demonstrates that the anomalous expansion observed is driven by the Poisson effect. In Fig. 1, only the radial lattice parameter has been included for the sake of clarity. The circumferential (tangential) lattice parameter (a_{circum}) can also be plotted as a function of the shell thickness and is expected to show a variation "inverse" to that observed for a_{radial}. This aspect is discussed in detail in the supplementary material (Section 2.1.2). Further, it is observed that Young's modulus does not have an effect on the a_{radial}, keeping other factors unchanged (see supplementary material, Section 2.1.1).

Fig. 2 shows the sample TEM micrographs of the MNS belonging to the lattice parameter expansion regimes (i.e., $a_{radial} > a_{bulk}^{Ni}$) and one micrograph of a nanoparticle, wherein lattice parameter contraction is observed. The dimensions of the nanostructures and the corresponding a_{radial} values obtained from the experiment and computation are as follows: (1) Nanoparticle (D = 6 nm): $a_{radial}^{exp} = 3.46$ Å and $a_{radial}^{comput} = 3.490$ Å; (2) thin walled MNS (OD = 150 nm, t = 25 nm): $a_{radial}^{exp} = 3.63$ Å and $a_{radial}^{comput} = 3.516$ Å, and (iii) very thin walled MNS (OD = 100 nm; t = 10 nm): $a_{radial}^{exp} = 3.81$ Å and $a_{radial}^{comput} = 3.524$ Å. Keeping in view that the OD and "t" are different in (ii) and (iii), it is seen that the expansion in the case of very thin walled MNSs (lying in regime-R3) is more than that of the thin walled MNS (lying in regime-R2). The experimental trendline corroborates well with the computational results, but the values obtained are higher. Experimentally, it is very difficult to control precisely and continuously the OD and "t" of the MNS and hence selected OD and shell thicknesses are chosen such that regions R2 and R3 are represented. To obtain good HRLFI, the thickness of a sample of 10 nm or less is preferred, and hence, it is very difficult to obtain LFI from MNS in region R3 (as discussed in the supplementary material, Section 1.2.2). This however does not pose a serious impediment to the conclusions drawn, as thick shells are similar to nanoparticles, wherein the outer surface stress dominates. An additional point in this regard is that a lattice contraction is to be expected in metal nanoparticles, and the regions R2 and R3 are of primary interest in the current work. It is noteworthy at this point that multiple factors make recording HRLFI of "ideal quality" very difficult (e.g., the stability of the particle under the electron beam and obtaining lattice fringes perpendicular to the radial direction within the thin shell). To obtain the best possible results and check the repeatability, multiple samples were synthesized and studied using TEM, and

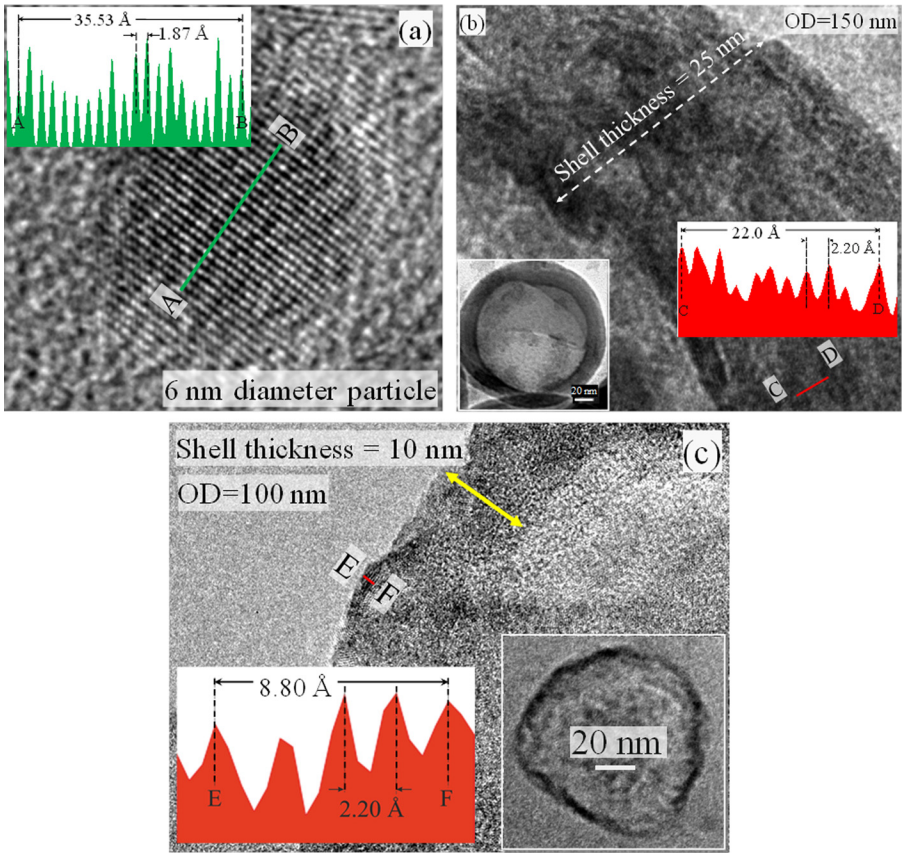

FIG. 2. Determination of interplanar spacing from high resolution lattice fringe images (HRLFI) for (a) a nanoparticle, (b) a thin shell (R2) MNS, and (c) a very thin shell (R3) MNS. The intensity patterns shown are across the lines in the HRLFI (AB, CD, and EF). The inset of figures (b) and (c) shows bright field images depicting the MNS studied.

additional results can be found in the supplementary material (Section 2.2).

In the present study, we have used Ni as an illustrative material. An interesting question at this juncture is: "is the phenomena observed specific to Ni or does it have a broader applicability?" To address this question, we focus our attention on elemental metals with low values of Poisson's ratio (ν). A few examples of these elements are[7] Be (HCP, $\nu \sim 0.02$), Te (HCP, $\nu = 0.16$), Cr (BCC, $\nu = 0.21$), and Th (CCP, $\nu = 0.26$). For further study, we choose Beryllium—an elemental metal with Poisson's ratio nearly zero. The interatomic spacing for a (111) monolayer of atoms of Be computed using DFT is 2.126 Å. Fig. 3 shows the variation in a_{radial} with "t" for a Be nanoshell with OD = 80 nm. An anomalous expansion region is observed in the figure (for $t < 5$ nm), establishing our confidence in the assertion that the phenomenon is reasonably widespread, if not universal for MNS. Our assertion that the phenomenon of anomalous expansion observed is Poisson effect driven is strengthened by contrasting the plots for Ni (Fig. 1) with Be (Fig. 3). Noteworthy differences are that (i) the effect of the inner surface stress is small for all values of "t," (ii) for $t > 5$ nm, the MNS behaves like a nanoparticle (i.e., lattice contraction, with $t_o^* = t_n^*$), and (iii) the anomalous lattice expansion region (R3) is considerably reduced (i.e., with lower Poisson's ratio, the anomalous effect is observed at lower "t"). One feature observed in the figure is that the lines for a_{bulk} and a_{inner} coincide. This is due to the fact that Poisson's ratio is nearly zero for Be, and to confirm this, the plot for a conceptual value of Poisson's ratio of 0.1 is included in the figure. It is seen that with $\nu = 0.1$, the previously observed behaviour (Fig. 1) is retrieved for small shell thicknesses. The insets of Fig. 3 show the stress state (plot of σ_{zz} obtained from the two-scale simulation) for a nanoshell (with $t = 10$ nm) and a nanoparticle (diameter of 80 nm). In the case of the nanoshell, the shell thickness is in the regime-R2 and the outer and inner surfaces are in tension, while the interior is under a variable compression. In contrast, in the case of the nanoparticle, the complete interior is in a state of uniform compression.

A few points noteworthy of attention with regard to the current work are as enumerated below: (1) Unlike pure continuum systems, the MNS have a fundamental length scale—the "thickness" of the surface layer. (2) The computational methodology used has its set of benefits and assumptions.

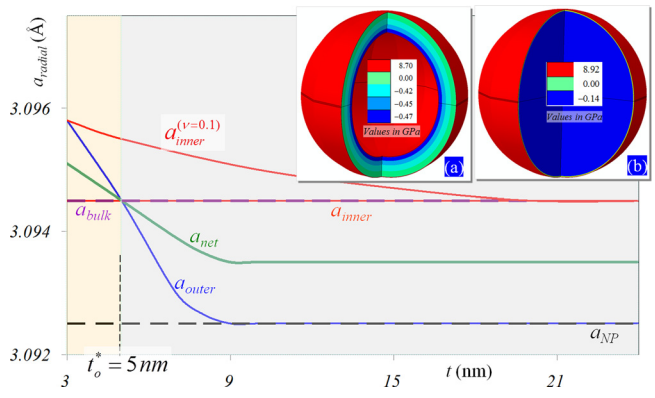

FIG. 3. Variation in the radial lattice parameters (a_{radial}, a_{outer}, a_{inner}, and a_{net}) with the shell thickness for a nanoshell of Be with OD = 80 nm computed using a two-scale method. It is to be noted that the lines for a_{inner} and a_{bulk} coincide. The curve of a_{radial} with $\nu = 0.1$ is also included for reference. The insets show the stress state (plot of σ_{zz}) of (a) a nanoshell with $t = 10$ nm and (b) a nanoparticle with 80 nm diameter.

Better models could capture the details better. (3) Local variations in the shell thickness, curvature, etc., are expected to influence the lattice parameter (measured using HRLFI). (4) Bulk properties have been used for the thin shells as well. In nanoscale materials, surface stress effects lead to altered properties,[26] which have been explicitly incorporated in the current simulations. (5) Although considerable care has been taken to avoid oxidation or contamination (during experimentation), these could be issues to some extent or the other. Oxidation will introduce a new surface layer and considerably alter the properties of the nanoparticle (including its effect on surface stresses).[27] (6) The polycrystallinity of the sample, which includes grain boundary stresses, may have to be accounted for to compute the accurate values of the lattice parameter. (7) The nanoshells synthesized in the current work represent a metastable state structurally and microstructurally. On annealing, the shells will tend towards becoming single crystals and may further undergo shape changes.

To summarize, we argue that a lattice expansion in the radial direction occurs in metal nanoshells due to purely surface stress effects. We discover that the Poisson effect drives the anomalous lattice expansion in very thin walled MNSs. Further, we demonstrate that this effect is expected to be widespread in the context of MNS. HRLFI in a TEM is used to measure this effect, and a two-scale simulation methodology is used to understand the origin of the same.

See supplementary material for details of the computational methodology, experimental techniques and results, and additional analysis (related to the effect of Young's modulus, variation in the circumferential lattice parameter, lattice parameter across the thickness).

The authors would like to thank Mr. M. Ambresh of Advanced Imaging Centre for help with TEM studies. Special thanks are due for Shilpi Saxena (Chemical Engineering, IITK) for help with synthesis of Ni hollow spheres.

[1]J. Woltersdorf, A. S. Nepjko, and E. Pippel, Surf. Sci. **106**, 64 (1981).
[2]A. M. Stoneham, J. Phys. C **10**, 1175 (1977).
[3]R. Lamber, S. Wetjen, and N. I. Jaeger, Phys. Rev. B **51**, 10968 (1995).
[4]W. H. Qi and M. P. Wang, J. Nano. Res. **7**, 51 (2005).
[5]S. Deshpande, P. Swanand, K. Kuchibhatla, and S. Sudipta, Appl. Phys. Lett **87**, 133113 (2005).
[6]P. M. Diehm, P. Ágoston, and K. Albe, ChemPhysChem **13**, 2443 (2012).
[7]W. F. Gale and T. C. Tottemeier, *Smithells Metals Reference Handbook* (Butterworth-Heinemann Publishers, Oxford, 2004).
[8]K. R. Olympio and F. Gandhi, J. Intell. Mater. Syst. Struct. **21**, 1737 (2010).
[9]R. H. Baughman, J. M. Skacklette, A. A. Zakhidev, and S. Stafström, Nature **392**, 362 (1998).
[10]L. Rothenburg, A. A. Berlin, and R. J. Bathurst, Nature **354**, 470 (1991).
[11]B. D. Caddock and K. E. Evans, J. Phys. D: Appl. Phys. **22**, 1877 (1989).
[12]I. B. Bischofs and U. S. Schwarz, Phys. Rev. Lett. **95**, 068102 (2005).
[13]J. B. Walsh, J. Geophys. Res. **70**, 5249, doi:10.1029/JZ070i020p05249 (1965).
[14]P. Tandaiya, U. Ramamurty, and G. Ravichandran, Acta Mater. **56**, 6077 (2008).
[15]X. X. Su, Y. F. Wang, and Y. S. Wang, Ultrasonics **52**, 255 (2012).
[16]C. P. Bergmann and F. M. Machado, *Carbon Nanomaterials as Adsorbents for Environmental and Biological Applications* (Springer International Publishing, New York, 2015).
[17]G. Zheng, S. W. Lee, Z. Liang, H.-W. Lee, K. Yan, H. Yao, H. Wang, W. Li, S. Chu, and Y. Cui, Nat. Nanotechnol. **9**, 618 (2014).
[18]J. Sun, J. Zhang, M. Zhang, M. Antonietti, X. Fu, and X. Wang, Nat. Commun. **3**, 1139 (2012).
[19]J. S. Cho, J. K. Lee, and Y. C. Kang, Sci. Rep. **6**, 23699 (2016).
[20]T. Vystavel, S. A. Koch, G. Palasantzas, and J. Th. M. De Hosson, Appl. Phys. Lett. **86**, 113113 (2005).
[21]T. Vystavel, G. Palasantzas, S. A. Koch, and J. Th. M. De Hosson, Appl. Phys. Lett. **82**, 197 (2003).
[22]T. Vystavel, G. Palasantzas, S. A. Koch, and J. Th. M. De Hosson, Appl. Phys. Lett. **83**, 3909 (2003).
[23]G. Iyer, D. De, A. Kumar, R. Pala, and A. Subramaniam, Appl. Surf. Sci. **371**, 343 (2016).
[24]R. Shuttleworth, Proc. Phys. Soc. A **63**, 444 (1950).
[25]M. E. Gurtin and A. Murdoch, Arch. Ration Mech. Anal. **57**, 291 (1975).
[26]J. Wang, H. L. Duan, Z. P. Huang, and B. L. Karihaloo, Proc. Roy. Soc. A **462**, 1355 (2006).
[27]S. A. Koch, G. Palasantzas, T. Vystavel, J. Th. M. De Hosson, C. Binns, and S. Louch, Phys. Rev. B **71**, 085410 (2005).